

1 Article

2 Optimal Routing for Time-Driven EH-WSN under 3 Regular Energy Sources

4 **Sebastià Galmés** ^{1,*}

5 ¹ Department of Mathematics and Computer Science, University of Balearic Islands, 07122 Palma de
6 Mallorca, Spain; sebastia.galmes@uib.es

7 * Correspondence: sebastia.galmes@uib.es; Tel.: +34-669-130-240

8 Received: date; Accepted: date; Published: date

9 **Abstract:** The recent provision of energy-harvesting capabilities to wireless sensor networks has
10 entailed the redefinition of design objectives. Specifically, the traditional goal of maximizing
11 network lifetime has been replaced by optimizing network performance, namely delay and
12 throughput. The present paper contributes to this reformulation by considering the routing
13 problem for the class of time-driven energy-harvesting WSN (EH-WSN) under regular or
14 quasi-periodic energy sources. In particular, this paper shows that the minimum hop count (MHC)
15 criterion maximizes the average duty cycle that can be sustained by nodes in this type of scenarios.
16 This is a primary objective in EH-WSN, since large duty cycles lead to enhanced performance.
17 Based on a previous result, a general expression is first obtained which gives mathematical form to
18 the relationship between duty cycle and traffic load for any node in a time-driven EH-WSN fed by
19 a regular energy source. This expression reveals that the duty cycle achievable by a node decreases
20 as its traffic load increases. Then, it is shown that MHC minimizes the average traffic load over the
21 network, and thus it maximizes the average duty cycle of nodes. This result is numerically
22 validated via simulation by comparison with other well-known routing strategies. Accordingly,
23 this paper suggests assigning top priority to the MHC criterion in the development of routing
24 protocols for time-driven EH-WSN under regular energy sources.

25 **Keywords:** energy-harvesting wireless sensor network; solar radiation; energy consumption
26 model; duty cycle; throughput; MAC layer; routing; minimum hop count; shortest-path routing
27

28 1. Introduction

29 Recent advances in wireless sensor networks have led to the development of energy-harvesting
30 capabilities, which are expected to enable very long or even perpetual operation. In parallel, the
31 design focus has progressively been shifted from maximizing network lifetime, usually defined as
32 the time until first node death, towards optimizing network performance, basically delay and
33 throughput [1]. So, despite energy issues in EH-WSN cannot be disregarded due to the time-varying
34 nature of ambient energy sources, the new design priorities demand for revising current protocols
35 for battery-powered WSN. Note that such new priorities represent a change in statistical sense too:
36 while the design goal in battery-powered WSN is to maximize a lower bound (time until first node
37 death), the goal in EH-WSN is to maximize an average (average performance). Such a difference
38 obviously conditions the design of protocols.

39 Most contributions on battery-powered WSN have focused on the MAC layer, as this plays a
40 fundamental role in the energy expended by a sensor node. Research activity on EH-WSN is also
41 giving priority to the development of MAC protocols, but relaxing the constraints on energy
42 consumption. Specifically, the new objective at the MAC layer is to increase the duty cycle of nodes
43 as much as possible according to their individual energy harvesting patterns, as opposed to the
44 common system-wide reduced duty cycle of battery-powered WSN. References [2-3] provide,

45 respectively, comprehensive surveys on MAC protocols for battery-powered and energy-harvesting
46 WSN.

47 The network layer is also under review. In fact, a few routing protocols for EH-WSN have been
48 recently proposed with the aim of optimizing performance metrics such as delay and throughput,
49 again in contrast to the network lifetime maximization pursued by traditional routing protocols
50 [4-5]. One of the contributions is [6], which proposes an algorithm rather than a protocol. This
51 algorithm, known as Energy-opportunistic Weighted Minimum Energy (E-WME), calculates the cost
52 of each node as an exponential function of its residual energy, and then uses shortest-path routing
53 on the basis of this metric. In addition, it offers high versatility, as it can be easily incorporated into
54 different routing implementation schemes, like proactive or on-demand. In [7], a modification on the
55 well-known Collection Tree Protocol (CTP) is proposed, namely Loop-aware CTP (La-CTP). This
56 protocol introduces several mechanisms to effectively suppress the occurrence of loops and unlock
57 unavoidable loops in moving packets across an EH-WSN. In general, these loops arise from
58 temporary departures of nodes that stop working to enter a recharging state. In [8], a hierarchical
59 topology is assumed and a centralized routing algorithm containing two parts is proposed. The first
60 part consists of a genetic-based unequal clustering algorithm, which is run by the base station to
61 form clusters of unequal size. Here, information about location, energy level and energy harvesting
62 rate of all nodes is used. After clustering, the base station executes another algorithm to construct an
63 inter-cluster routing among all cluster heads. This algorithm also takes into account the energy
64 harvesting condition of the participant nodes, in this case the cluster heads. Another contribution is
65 [9], which proposes the Energy Harvesting Opportunistic Routing (EHOR) protocol for multi-hop
66 EH-WSN. This kind of opportunistic protocol uses a region-based approach to determine the
67 optimal forwarders for every packet, by taking into account the energy condition of all nodes, and
68 the fact that some of them are in recharging state and thus they are temporally unavailable. In [9], a
69 linear topology is assumed. Then, EHOR is extended to 2D topologies in [10], under the name of
70 AOR (Adaptive Opportunistic Routing). Finally, [11] and [12] propose modifications on LEACH
71 [13], which is the most well-known hierarchical protocol for battery-powered sensor networks.
72 Particularly, an Energy Potential (EP) function is introduced in [11] to quantify the node capability of
73 energy harvesting. The resulting protocol, called EP-LEACH, uses the EP function in the cluster
74 head selection strategy. Compared to LEACH, it is shown to exhibit better performance in terms of
75 lifetime and throughput. A similar approach is followed in [12], but in this case a solar energy
76 prediction model based on a neural network is used to estimate the energy that is to be harvested by
77 a node in a short term horizon. This estimate and the node current residual energy are then
78 combined to determine the probability of the node to become a cluster head. Again, simulation
79 results demonstrate that the proposed clustering method outperforms that of traditional LEACH
80 with respect to average residual energy of nodes and network throughput.

81 A common characteristic to the above routing protocols (except La-CTP) is that they assume an
82 oversimplified MAC layer, where the only sources of energy consumption are the pure transmission
83 and reception of packets. Whereas this is true for TDMA-based MAC protocols, it is far from reality
84 for the rest of them, since they typically involve other sources of energy expenditure, namely idle
85 listening, packet retransmissions, etc. Another drawback of current routing protocols for EH-WSN is
86 their reliance on heuristic algorithms, which do not necessarily lead to optimal performance and/or
87 incur significant overhead in terms of computational time or control traffic. Whereas these
88 approaches may constitute the only viable methodology for EH-WSN subject to unpredictable traffic
89 loads and/or energy sources, the regular patterns exhibited by some energy-harvesting processes,
90 like those based on solar power, and some traffic loads, like those resulting from periodic
91 monitoring applications, suggest the possibility of analytical treatment.

92 This paper focuses on EH-WSN devoted to periodic monitoring, also known as time-driven
93 EH-WSN. Under the time-driven paradigm, nodes periodically sense the environment and report
94 the corresponding data to the base station, usually via multi-hop communication. This is the case of
95 numerous sensor-based applications, which span a great diversity of monitored variables. Typically,
96 the design of the MAC layer is based on duty-cycling the communication activity of nodes, in order

97 to avoid fast depletion of energy resources due to idle listening. Since the reporting frequencies
98 imposed by monitoring applications are commonly very low, every reporting period may contain
99 thousands of unused duty cycles due to the relatively small number of packets being transmitted or
100 forwarded. Therefore, in spite of having duty-cycled the communication activity, idle listening is
101 still a dominant component in the energy wasted by time-driven sensor networks. Note that this is
102 true for both, battery-powered and energy-harvesting sensor networks, though it is expected that
103 the latter allow for larger duty cycles, or for larger network sizes under the same duty cycle.

104 Particularly, the present work follows an analytical approach to address the routing problem in
105 time-driven (duty-cycled) EH-WSN operating under regular or quasi-periodic energy sources,
106 among which solar radiation is the most representative example. Such approach relies on a
107 comprehensive energy consumption model for the MAC layer, which takes into account all sources
108 of energy consumption, and on the application of the so-called energy neutral condition for
109 EH-WSN. The following assumptions are adopted:

- 110 • Both planar and hierarchical topologies are taken into account. In the latter case, the routing
111 problem focuses on interconnecting the cluster heads to the base station.
- 112 • At most, data aggregation is considered at the intra-cluster level in the case of hierarchical
113 topologies. This is consistent with the trend of deploying sensor networks over larger and
114 larger areas, fact that reduces correlation among data from different sub-regions.
- 115 • Homogeneous distribution of the traffic workload generated by nodes (offered traffic). This
116 means that all sensor nodes generate the same amount of packets per unit of time.
- 117 • The transmit power of nodes is set to the maximum, that is, power control is disabled. This
118 implies that the energy wasted by a node to transmit a packet does not depend on distance,
119 except for the fact that the receiving node must be located within its transmission range.

120 On the basis of these assumptions, this paper demonstrates that the MHC criterion should be
121 prioritized in the design of routing strategies and protocols for time-driven EH-WSN under regular
122 energy sources. More specifically, the detailed contributions of this paper can be outlined as follows:

- 124 • Based on a previous result about the energy consumed by TinyOS sensor nodes [14], a
125 comprehensive model is derived to characterize the energy consumption of nodes in generic
126 time-driven duty-cycled wireless sensor networks.
- 127 • A general formulation is then obtained which relates duty cycle and traffic load in time-driven
128 duty-cycled EH-WSN.
- 129 • It is mathematically shown that, in addition to the obvious minimization of path delay, the
130 minimum hop count criterion also minimizes the average traffic load over the network, and
131 thus it maximizes the average duty cycle of nodes. In turn, this contributes to minimizing the
132 link-level delay and maximizing the average network throughput that can be sustained by the
133 whole network.

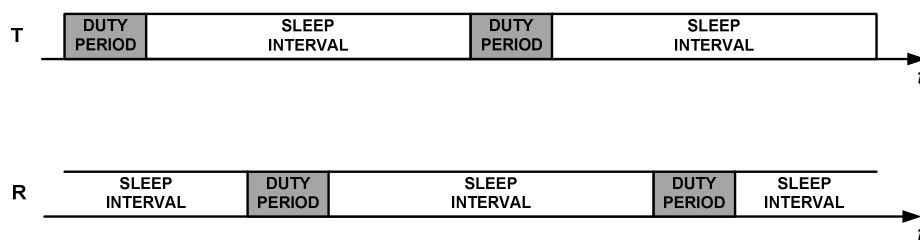
134 The rest of this paper is organized as follows. In Section 2, from the result obtained in [14], a
135 generic energy consumption model for time-driven duty-cycled sensor networks is developed. By
136 assuming a regular or quasi-periodic energy source, the condition for energy neutral operation is
137 reformulated in Section 3. In Section 4, it is shown that the MHC metric minimizes the average traffic
138 load over the network and maximizes the average duty cycle of nodes. In Section 5, numerical
139 results are obtained and compared with those from other routing metrics. Some remarkable
140 differences between applying the MHC criterion to energy-harvesting and battery-powered sensor
141 networks are highlighted in Section 6. Finally, Section 7 concludes the paper with suggestions for
142 further research.

143 2. Energy Consumption Model

144 There are two types of duty-cycled MAC protocols in sensor networks, namely synchronous
145 and asynchronous. Synchronous protocols are based on TDMA and thus represent an extreme case
146 of duty-cycling, since nodes are only active during the specific timeslots devoted to transmit or

147 receive. This results from the fact that any transmitter and its receiver wake up at the same time.
 148 However, such protocols require tight synchronization among nodes, and exhibit significant
 149 limitations in terms of scalability and adaptiveness to changing traffic conditions. These
 150 disadvantages make asynchronous protocols more attractive, at the expense of more energy
 151 consumption and some throughput degradation.

152 In asynchronous communication, nodes have their duty cycles completely decoupled, as it is
 153 shown in Figure 1. Thus, two general mechanisms have been proposed in literature in order to link a
 154 transmitter that has data to send with its receiver: Low Power Listening (LPL) and Low Power
 155 Probing (LPP). In LPL, the responsibility of the task is shifted to the transmitter, which uses a duty
 156 period to initially send a long preamble or a burst of advertisement packets in order to warn the
 157 receiver that it has pending data. It can also send a repetitive sequence of the data packet itself. Upon
 158 waking up and detecting the preliminary signalling or the sequence of data packets, the receiver
 159 stays awake until the transmission process is completed, meaning that a full data packet has been
 160 correctly received. Examples of implementations of LPL are X-MAC [15], Aloha with preamble
 161 sampling [16], B-MAC [17], and BoX-MAC-1 and BoX-MAC-2 [18]. In contrast, in LPP [19], it is the
 162 receiving node that periodically sends small packets called beacons or probes, to announce that it is
 163 awake and ready to receive data. A node willing to send a packet turns its radio on and waits for a
 164 probe. Upon receiving a probe from the intended destination, it sends an acknowledgment and,
 165 subsequently, the data packet. The most representative LPP protocols are RI-MAC [20] and A-MAC
 166 [21].



167

168 **Figure 1.** Uncoupled duty cycles between a transmitter node (T) and a receiver node (R) in
 169 asynchronous communication.

170 As stated above, both synchronous and asynchronous mechanisms are part of the class of
 171 duty-cycled MAC protocols, as in both cases nodes use non-activity periods to switch to sleep mode
 172 in order to save energy. However, usually the term duty-cycled MAC protocol refers to the
 173 asynchronous version, which is the most extended implementation [22]. This is the focus of the
 174 present paper.

175 2.1 Energy Consumption Model for the LPL mechanism in TinyOS Sensor Nodes

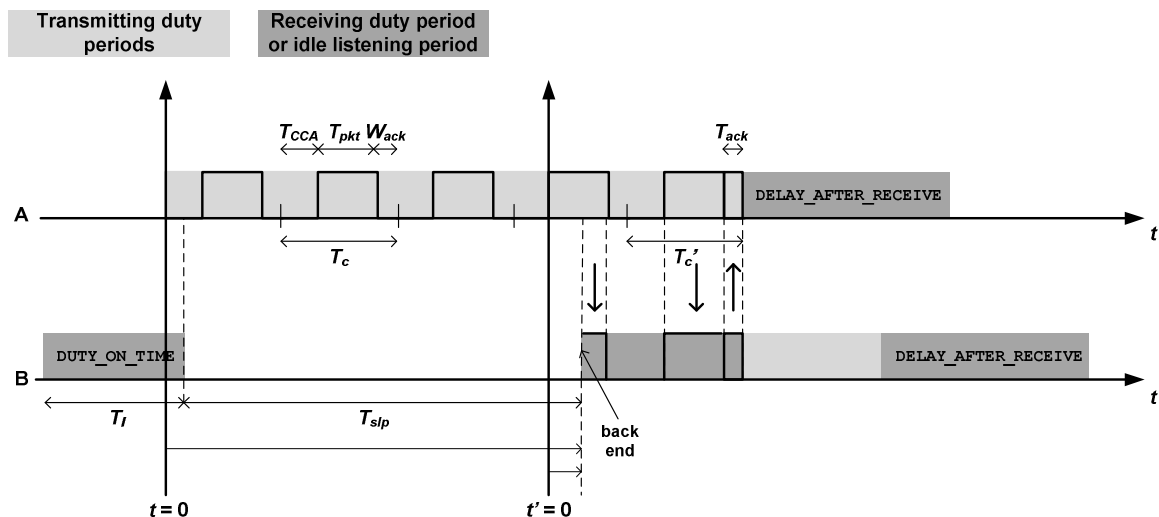
176 For the sake of completeness, this subsection recalls the main results obtained in [14] about the
 177 energy consumed by the LPL mechanism implemented in TinyOS sensor nodes. Figure 2 describes
 178 this mechanism, where node A transmits a packet to node B, which receives and forwards such
 179 packet to the next hop (not shown). As it can be noticed, node A sends the packet repetitively until
 180 node B wakes up, captures the full packet and sends back an acknowledgment packet. The figure
 181 introduces the following temporal magnitudes:

- 182 • T_{CCA} : Time for clear channel assessment. This is the time required by the sending node to check
- 183 that there are no ongoing transmissions on the channel.
- 184 • T_{pkt} : Packet duration.
- 185 • W_{ack} : Waiting time for the acknowledgment from the receiver. If no acknowledgment is
- 186 received, the transmission was unsuccessful and the transmitter tries again.
- 187 • T_{ack} : Duration of acknowledgment packets.
- 188 • $T_c = T_{CCA} + T_{pkt} + W_{ack}$.
- 189 • $T_c' = T_{CCA} + T_{pkt} + T_{ack}$.

- 190 • T_l : Nominal duration of duty periods, also known as DUTY_ON_TIME in TinyOS nomenclature.
 191 This is, in fact, the duration of duty periods in absence of traffic activity (minimum duration).
 192 • T_{slp} : Duration of sleep periods. If DC denotes the nominal duty cycle (in percentage), we can
 193 set up the following equality: $DC = \frac{T_l}{T_l + T_{slp}} \cdot 100$.
 194 • DAR : This is the DELAY_AFTER_RECEIVE, a period of time that a node remains active after
 195 completing a traffic task, either a transmission (node A) or a reception (with subsequent
 196 forwarding) (node B). Note that the name of this magnitude does not reflect its full role, as it
 197 suggests that it only takes place after a packet reception.

198 According to the assumption that the offered traffic is homogeneously distributed over the
 199 network (Section 1), let us assume, with no loss of generality, that each node reports one packet per
 200 communication round. Therefore, if a given node X has $\sigma(X)$ descendants in the routing tree, its
 201 traffic load is precisely $\sigma(X)$, since this node has to receive and forward $\sigma(X)$ packets (aside from
 202 transmitting its own packet). In [14], an accurate expression is provided for the energy consumed by
 203 a TinyOS sensor node in every communication round of a time-driven application:

$$\varepsilon[E_{round}(X)] = \sigma(X) \cdot \varepsilon[E_R(X)] + (\sigma(X) + 1) \cdot \varepsilon[E_T(X)] + \left(\frac{T_{rnd}}{T_l + T_{slp}} - (\sigma(X) + 1) \right) \cdot E_l \quad (1)$$



204
 205
 206

Figure 2. Operation of LPL in TinyOS sensor nodes: node A transmits a packet to node B, which receives and forwards this packet.

207 In the above equation, $E_R(X)$ denotes the energy wasted to receive a packet, $E_T(X)$ is the
 208 energy wasted to transmit a packet, T_{rnd} is the duration of a communication round and E_l is the
 209 energy consumed in idle listening by every duty period without traffic activity. $\varepsilon[\cdot]$ is the
 210 expectation operator. The presence of this operator is due to the random asynchrony between the
 211 duty periods of the two communicating nodes (see Figure 2). This randomness is reflected in two
 212 components: the number of tries performed by the transmitter until it receives an acknowledgment
 213 (node A in Figure 2), and the fraction of receiver duty period until the start of a full packet (node B in
 214 Figure 2). Specifically, the two expectations in Equation (1) can be formulated as follows:

$$\varepsilon[E_T(X)] = (\varepsilon[k] - 1) \cdot E_c(X) + E_c'(X) + E_l^{DAR} \quad (2)$$

$$\varepsilon[E_R(X)] = \varepsilon[E_{fd}] + E_{rx}^{pkt} + E_{tx}^{ack} \quad (3)$$

215 In these equations, $\varepsilon[k]$ and $\varepsilon[E_{fd}]$ are, respectively, the expected number of tries and the
 216 expected duration of a fragment of duty period, $E_c(X)$ is the energy wasted in non-successful
 217 transmission cycles, whose duration is T_c , and $E_c'(X)$ is the energy wasted in a successful
 218 transmission cycle, the duration of which is T_c' (Figure 2). Additionally, E_l^{DAR} , E_{rx}^{pkt} and E_{tx}^{ack} are,
 219 respectively, the energy consumed in a DELAY_AFTER_RECEIVE period, the energy wasted to

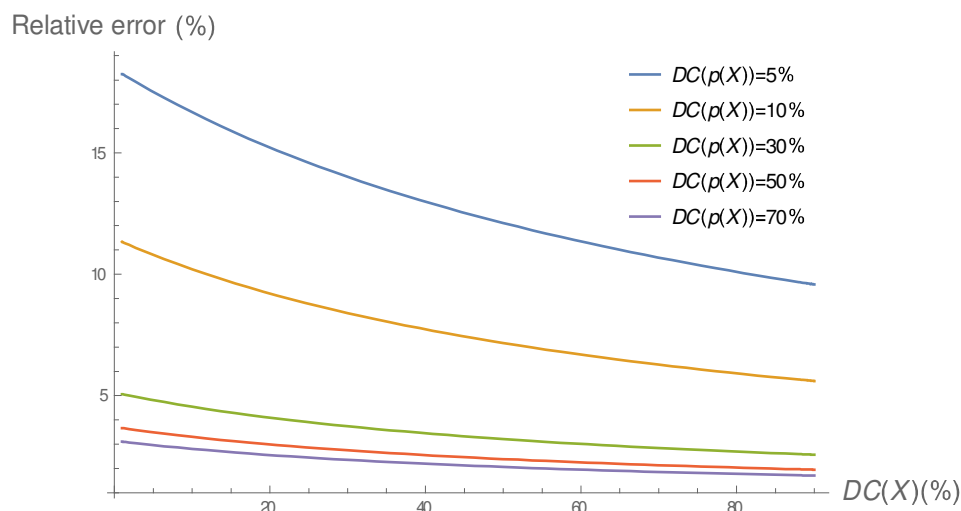
220 receive a packet and the energy wasted to transmit an acknowledgment. Note that, implicitly, it has
 221 been assumed that power control is disabled, because the energy wasted to transmit an
 222 acknowledgment, which is part of the energy wasted to receive a packet, does not exhibit any
 223 dependence on the specific node to which the acknowledgment is sent. This is reflected in the fact
 224 that the traffic load generated by all descendants of node X has been grouped into a single term
 225 $\sigma(X)$ in Equation (1). Whereas this contributes to simplifying the analysis it does not cause any
 226 detriment on the generality of subsequent results.

227 2.2 Approximate Energy Consumption Model

228 In this subsection, the model just described is generalized to any implementation of LPL or LPP.
 229 To start with, Equation (1) can be simplified by removing several terms that are very specific to the
 230 implementation of LPL in TinyOS and do not have significant contribution. Accordingly, the
 231 following approximate energy consumption model can be derived:

$$\begin{aligned} \varepsilon[E_{round}(X)] &\cong \sigma(X) \cdot E_{rxpkt} \\ &+ (\sigma(X) + 1) (\varepsilon[k] \cdot E_{txpkt} + E_l^{DAR}) + E_l \frac{T_{rnd} DC(X)}{T_l 100} \end{aligned} \quad (4)$$

232 In this equation, it has also been assumed that the number of duty cycles per communication
 233 round is very large compared to the amount of such duty cycles that are entailed to transmit or
 234 receive. This assumption is in agreement with the large reporting periods that typically characterize
 235 time-driven applications, though again it does not compromise the generality of the main results of
 236 this paper. The term $DC(X)$ denotes the duty cycle of node X (expressed in percentage). On the
 237 other hand, the term $\varepsilon[k]$ depends on the duty cycle of the parent node of node X , namely
 238 $DC(p(X))$. In effect, as it can be noticed from Figure 2, it is the dynamics of node B that determines the
 239 number of tries required by node A. The specific relationship between $\varepsilon[k]$ and $DC(p(X))$ for
 240 TinyOS nodes can be found in [14], but it has been omitted here as it is not relevant to the analysis
 241 that follows.



242
 243 **Figure 3.** Relative error between exact and approximate energy consumption models for TinyOS
 244 sensor nodes.

245 Figure 3 shows the relative error between the exact model, given by Equation (1), and the
 246 approximate model given by Equation (4), in terms of $DC(X)$, for different values of $DC(p(X))$. The
 247 rest of parameters are given in Table 1. As it can be noticed, the relative error decreases as both duty
 248 cycles increase. Particularly, for duty cycles equal to or larger than 40%, the relative error is around
 249 2%. As stated in Section 1, large (and heterogeneous) duty cycles are very common in EH-WSN, and
 250 thus the approximate energy consumption model can replace the exact one for TinyOS EH-WSN.

251 To proceed with the generalization, we can start by reformulating Equation (4) as follows:

$$\begin{aligned} \varepsilon[E_{round}(X)] &\cong \sigma(X) \cdot E_{rxpkt} + (\sigma(X) + 1) \cdot E_{txpkt} \\ &+ E_l \frac{T_{rnd} DC(X)}{T_l 100} + (\sigma(X) + 1) \cdot E_{trigger}(X) \end{aligned} \quad (5)$$

252 Here, $E_{trigger}(X)$ represents the energy wasted by the transmitter (node X) to trigger the
253 communication with its receiver (node $p(X)$). For TinyOS nodes, it can be expressed as follows,
254 where $\varepsilon[n]$ denotes the expected number of (unsuccessful) transmission tries before a correct data
255 packet is received:

$$E_{trigger}(X) = \varepsilon[n]E_{txpkt} + E_l^{DAR} \quad (6)$$

256 **Table 1.** Parameters used in the validation of the approximate energy consumption model for LPL
257 TinyOS nodes.

Magnitude	Value
Bandwidth	250 Kbps
T_{pkt}	1.312 ms
T_{ack}	0.544 ms
T_{CCA}	0.4 ms
W_{ack}	1 ms
T_l	5 ms
DAR	100 ms
T_{rnd}	60 s
Voltage	3 V
Current draw in RX	18.8 mA
Current draw in TX (at 0 dBm)	17.4 mA

258 A detailed analysis of Equation (5) reveals that all terms except the last one characterize the
259 main sources of energy consumption in any time-driven duty-cycled sensor network, regardless of
260 the particular platform. At the same time, specific implementation details about the triggering
261 method can be assumed to be embedded into the variable $E_{trigger}(X)$. Accordingly, Equation (5)
262 becomes appropriate to model a large variety of LPL and even LPP-based MAC protocols, and hence
263 it can be used to formulate the condition for energy neutral operation in the next section. For the
264 sake of completeness, we can attempt to infer a more explicit but still general formulation for
265 $E_{trigger}(X)$. In the case of LPL-based MAC protocols, the following expression can be postulated:

$$E_{trigger}(X) = \begin{cases} \varepsilon[n]E_{txpkt} + E_{extra}, & \text{case 1} \\ \varepsilon[n]E_{txadv} + E_{extra}, & \text{case 2} \\ \varepsilon[E_{fp}] + E_{extra}, & \text{case 3} \end{cases} \quad (7)$$

266 Here, cases 1, 2 and 3 correspond, respectively, to using a repetitive sequence of the data packet
267 (LPL in TinyOS), a repetitive sequence of an advertisement packet or a long preamble. Moreover,
268 $\varepsilon[n]$ denotes the expected number of times that the data packet or the advertisement packet is
269 transmitted before the data packet is fully received, $\varepsilon[E_{fp}]$ is the expected value of energy wasted in
270 transmitting a fragment of preamble and E_{extra} stands for any extra fixed-component of energy
271 consumption that may be introduced by the particular MAC protocol (for instance, E_l^{DAR} in
272 TinyOS).

273 In the case of LPP-based protocols, where typically a probe packet is repetitively transmitted by
274 the node acting as receiver, the formulation is slightly different:

$$\begin{aligned} \varepsilon[E_{round}(X)] &\cong \sigma(X) \cdot E_{rxpkt} + (\sigma(X) + 1) \cdot E_{txpkt} \\ &+ E_l \frac{T_{rnd} DC(X)}{T_l 100} + \sigma(X) \cdot E_{trigger}(X) \end{aligned} \quad (8)$$

$$\begin{aligned}
 E_{trigger}(X) &= \sum_{i=1}^{CH(X)} \frac{\sigma(c_i(X))}{\sigma(X)} \cdot E_{trigger,i}(X) \\
 &= \sum_{i=1}^{CH(X)} \frac{\sigma(c_i(X))}{\sigma(X)} \cdot (\varepsilon_i[n]E_{txprobe} + E_{extra})
 \end{aligned} \tag{9}$$

275 The term $c_i(X)$ represents a child node of node X , with i varying between 1 and $CH(X)$, the
 276 total number of children of node X , and $\varepsilon_i[n]$ is the expected number of transmissions of the probe
 277 packet from node X to node $c_i(X)$. The term $E_{trigger,i}(X)$ denotes the energy wasted by node X to
 278 trigger the communication from its child node $c_i(X)$. Also note that $\sigma(X) = \sum_{i=1}^{CH(X)} \sigma(c_i(X))$, with
 279 $\sigma(c_i(X))$ the traffic load of node $c_i(X)$. Hence, Equation (9) can be viewed as a weighted average.

280 Equations (5) and (8) can be assimilated into the following equation, since the reporting time is
 281 always much larger than the duration of duty periods ($\frac{T_{rnd}}{T_l} \gg 1$):

$$\begin{aligned}
 \varepsilon[E_{round}(X)] &\cong \sigma(X) \cdot (E_{rxpkt} + E_{txpkt} + E_{trigger}(X)) \\
 &\quad + E_l \frac{T_{rnd}}{T_l} \frac{DC(X)}{100}
 \end{aligned} \tag{10}$$

282 In summary, Equation (10) characterizes, in an approximate way, the energy consumption (per
 283 round) of nodes in time-driven WSN implementing LPL-based or LPP-based duty-cycled MAC
 284 protocols. Whereas the specificity of the MAC protocol is embedded into the term $E_{trigger}(X)$, the
 285 important fact regarding the subsequent analysis is the dependence of the energy consumption per
 286 round on the traffic load, represented by $\sigma(X)$. Next, based on Equation (10), the condition for
 287 energy neutral operation is formulated.

288 3. Energy Neutral Operation

289 In contrast to conventional battery-powered WSN, which are designed with the objective of
 290 maximizing network lifetime, in the case of EH-WSN, the objective is to maximize performance
 291 under self-sustained operation. More formally, this condition is known as energy neutral operation
 292 (ENO), which essentially means that, in a given period of time, the energy balance at a node is
 293 non-negative. Also, many energy-harvesting mechanisms in sensor networks obey the so-called
 294 harvest-store-consume supply alternative, which consists of combining the energy-harvesting
 295 subsystem with a buffer for energy storage (rechargeable battery or supercapacitor) [3]. According
 296 to this model, and assuming that the energy buffer does not have any inefficiency in charging and
 297 does not leak any energy over time, ENO can be mathematically formulated as follows [23] (the
 298 notation has been adapted):

$$E(t) = E(0) + \int_0^t P_{out}(u) du - \int_0^t P_c(u) du \geq 0, \forall t \geq 0 \tag{11}$$

299 In this expression, $E(t)$ denotes the energy balance at time t , $P_{out}(t)$ is the output power
 300 delivered by the harvesting subsystem at time t , $P_c(t)$ is the power consumed by the device at time
 301 t and, obviously, $E(0)$ is the energy initially stored in the buffer. Let us assume that the energy
 302 source exhibits a regular pattern, with periodicity T_S (energy-harvesting period). Accordingly, ENO
 303 can be formulated for one period T_S , since this is typically a very large multiple integer of the
 304 reporting period given by T_{rnd} . For instance, the most representative periodic source is the sunlight
 305 (really, it is quasi-periodic, but this will be considered further), as photovoltaic circuits constitute the
 306 most efficient form of energy conversion, at least for current sensor networks. In this case, T_S
 307 corresponds to one-day interval, which is much larger than usual reporting periods (one or several
 308 minutes). For the same reason, we can undoubtedly assume that the energy consumed by the sensor
 309 node is uniformly distributed over the round duration, implying that power consumption is
 310 independent of time: $P_c(t) = P_c = \frac{E_{round}}{T_{rnd}}$. Under these assumptions, ENO can be reformulated for a

311 given node X by imposing that the energy at the beginning of an energy-harvesting period is equal
 312 to the energy at the beginning of the previous energy-harvesting period:

$$E(T_S, X) = E(0, X) + \int_0^{T_S} P_{out}(u, X) du - \int_0^{T_S} \frac{E_{round}(X)}{T_{rnd}} du = E(0, X) \quad (12)$$

313 Note that, in order to guarantee that $E(t, X) \geq 0 \forall t$, a condition on $E(0, X)$ (initial energy) must
 314 also be fulfilled. Moreover, sufficiently large values of $E(0, X)$ release nodes from the need to enter a
 315 recharging state, even if significant irregularities occur during the energy-harvesting process (for
 316 instance, cloudy days in the case of solar-based sensor networks). However, despite the importance
 317 of $E(0, X)$ as an energy repository that mitigates the irregularities of the energy sources considered
 318 in this paper, its mathematical formulation has been omitted here as it is not relevant to the
 319 subsequent analysis. Then, by combining equations (10) and (12), we can end up with the following
 320 expression for the duty cycle of node X in terms of its energy harvesting capability and traffic load:

$$\frac{DC(X)}{100} \cong \frac{E_{out}(T_S, X) T_l}{E_l T_S} - \sigma(X) \cdot \frac{E_{rxpkt} + E_{txpkt} + E_{trigger}(X) T_l}{E_l T_{rnd}} \quad (13)$$

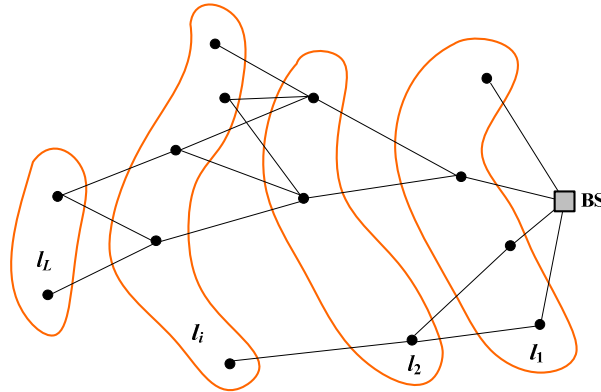
321 Here, $E_{out}(T_S, X) = \int_0^{T_S} P_{out}(u, X) du$. Equation (13) extends the ENO condition obtained in [14]
 322 to regular energy sources and generic duty-cycled MAC protocols. It makes it explicit the
 323 dependence of the duty cycle on the specific operating conditions of each node in the network,
 324 namely energy harvesting capability and traffic load. In particular, the presence of the energy
 325 harvesting term contributes to achieving much larger duty cycles in EH-WSN than those obtained in
 326 battery-powered WSN. Besides, Equation (13) reveals that the duty cycle decreases as the traffic load
 327 increases.

328 4. Criterion for Optimal Routing

329 It is well known that, in EH-WSN, enhancing performance under self-sustained operation
 330 implies maximizing the duty cycle of nodes as much as possible. According to expression (13),
 331 maximizing the duty cycle of any node requires minimizing its traffic load (for the rest of parameters
 332 remaining fixed). However, reducing the traffic load of a node may be achieved at the expense of
 333 increasing the traffic load of nearby nodes. So, the emphasis will be put on the average traffic load
 334 across the network. In a global sense, minimizing the average traffic load across the sensor network
 335 will contribute to maximizing the average duty cycle of nodes, fact that in turn will contribute to
 336 improve performance metrics.

337 The problem of minimizing the average traffic load can be addressed by decomposing the
 338 sensor network into layers. Let us assume that the transmission range of all nodes is r , and let us
 339 define l_1 as the subset of nodes that are at a distance not greater than r from the base station. Next,
 340 let us define l_2 as the subset of nodes that are in the transmission range of at least one node in l_1
 341 but at a distance greater than r from the base station, l_3 as the subset of nodes that are in the
 342 transmission range of at least one node in l_2 but out of the transmission range of all nodes in l_1 , and
 343 so on. In this layer decomposition process, it is assumed that a layer exists if it contains at least one
 344 element (node), and that the existence of layer l_i implies the existence of layer l_{i-1} , for any
 345 $i = 2 \dots L$. Figure 4 shows an example of layer decomposition for a connected network. Note that, if
 346 N is the number of sensor nodes in the network and L is the number of (non-empty) layers, the
 347 following properties hold:

- 348 • $L \leq N$. The equality corresponds to the case where each layer contains a single node.
- 349 • $l_i \cap l_j = \emptyset, \forall i \neq j$. This property is a direct consequence of the definition of layer.
- 350 • If the network is connected, $l_1 \cup l_2 \cup \dots \cup l_L = u$, where u represents the set of all sensor nodes.
- 351 • If the network is disconnected, $l_1 \cup l_2 \cup \dots \cup l_L \subset u$.



352

353 **Figure 4.** Layer decomposition of a connected network. Lines represent feasible links for the given
 354 transmission range. Only inter-layer links are drawn.

355 Once it has been verified that the network is connected, the next step is to find an appropriate
 356 routing topology. In our context, this means determining a spanning tree rooted at the base station
 357 that minimizes the average traffic load across the network. To achieve this goal, let us first define n_i ,
 358 with $i = 1 \dots L$, as the size of layer l_i , that is, the number of nodes contained in this layer. Obviously,
 359 $\sum_{i=1}^L n_i = N$. If we assume, with no loss of generality, that each node sends one packet per reporting
 360 period, then the traffic load supported by node x_k , namely $\sigma(x_k)$, $k = 1 \dots N$, is the total number of
 361 descendants of this node in the spanning tree. Let us also assume that only inter-layer connections
 362 (directed towards the base station) are allowed. In this case, the following lemma holds:

363 **Lemma 1.** If $\bar{\sigma}$ denotes the average traffic load supported by a network that only contains
 364 inter-layer connections, the following equation holds: $\bar{\sigma} = \frac{1}{N} \sum_{i=1}^{L-1} \sum_{j=i+1}^L n_j$, with n_j the size of layer
 365 l_j , $j = 1 \dots L$.

366 *Proof:* Let $\bar{\sigma}_i$ be the average traffic load supported by nodes in layer l_i , $i = 1 \dots L$. Then, $\bar{\sigma}_L = 0$
 367 and $\bar{\sigma}_i = \frac{\sum_{j=i+1}^L n_j}{n_i}$, $i = 1 \dots L - 1$. The first part of the statement is obvious, since $\sigma(x_k) = 0 \forall x_k \in l_L$
 368 (nodes in the last layer do not receive packets from other nodes). For the second part, let us first
 369 consider layer l_{L-1} . In this case, regardless of the specific inter-layer connections between this layer
 370 and layer l_L , we have $\sum_{x_k \in l_{L-1}} \sigma(x_k) = n_L$: since all input links to nodes in layer l_{L-1} come from
 371 nodes in layer l_L , and each node generates one packet per reporting period, the overall traffic load
 372 carried out by layer l_{L-1} coincides with the number of nodes in layer l_L . Accordingly, the average
 373 traffic load supported by layer l_{L-1} is $\bar{\sigma}_{L-1} = \frac{\sum_{x_k \in l_{L-1}} \sigma(x_k)}{n_{L-1}} = \frac{n_L}{n_{L-1}}$. Next, since all input links to nodes
 374 in layer l_{L-2} come from nodes in layer l_{L-1} , we can state that $\sum_{x_k \in l_{L-2}} \sigma(x_k) = \sum_{x_k \in l_{L-1}} (1 + \sigma(x_k))$,
 375 because each node $x_k \in l_{L-1}$ generates one packet and forwards a number of packets equal to its
 376 traffic load. Moreover, we can state that $\sum_{x_k \in l_{L-1}} (1 + \sigma(x_k)) = n_{L-1} + \sum_{x_k \in l_{L-1}} \sigma(x_k) = n_{L-1} + n_L$,
 377 which means that, with only inter-layer connections, the traffic load supported by layer l_{L-2} is equal
 378 to the total number of nodes in layers l_{L-1} and l_L . In turn, this implies that the average traffic load
 379 supported by nodes in layer l_{L-2} is given by $\bar{\sigma}_{L-2} = \frac{n_{L-1} + n_L}{n_{L-2}}$. So, from the point of view of layer l_{L-2} ,
 380 all nodes in layers l_{L-1} and l_L can be grouped into a single $l_{L-1} \cup l_L$ super-layer. Then, by iterating
 381 this procedure over subsequent layers, we can end up with a general expression for the average
 382 traffic load supported by a any layer: $\bar{\sigma}_i = \frac{\sum_{j=i+1}^L n_j}{n_i}$, $i = 1 \dots L - 1$. Finally, the average traffic load
 383 supported by the entire network can be expressed as $\bar{\sigma} = \sum_{i=1}^L \bar{\sigma}_i \cdot \frac{n_i}{N} = \frac{1}{N} \sum_{i=1}^{L-1} \sum_{j=i+1}^L n_j$. *qed*

384 The following lemma demonstrates that a routing tree based exclusively on inter-layer
 385 connections minimizes the average traffic load:

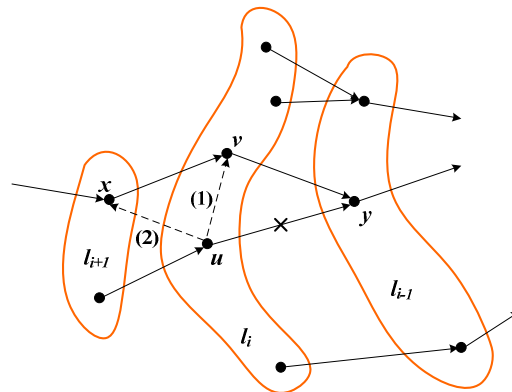
386 **Lemma 2.** Let $\bar{\sigma}^{(c)}$ the average traffic load that results from applying a given routing criterion
 387 c to construct the spanning tree. If $\bar{\sigma}^*$ denotes the average traffic load obtained by applying the

388 “only inter-layer connections” criterion, the following statement is true: $\bar{\sigma}^* = \min_{c \in C} \{\bar{\sigma}^{(c)}\}$, with C
 389 the set of all possible criteria.

390 *Proof.* In general, any routing criterion different from “only inter-layer connections” will give
 391 rise to at least $L - 1$ inter-layer connections (as there must be at least 1 inter-layer connection
 392 between two successive layers) combined with several intra-layer and/or backward inter-layer
 393 connections (see Figure 5). Let us first focus only on intra-layer connections. Figure 5 shows the
 394 simplest variation that can be introduced into a spanning tree that initially contains inter-layer
 395 connections exclusively. As it can be noticed, node u belonging to layer l_i is reconnected to node v
 396 in the same layer. The new connection, labeled (1), only causes an increase in the traffic load
 397 supported by node v . In effect, if $\sigma_{old}(x_k)$ and $\sigma_{new}(x_k)$ denote, respectively, the traffic load of any
 398 given node x_k before and after the reconnection, we have:

- 399 • $\sigma_{new}(u) = \sigma_{old}(u) = \sigma(u)$.
 400 • $\sigma_{new}(v) = \sigma_{old}(v) + 1 + \sigma(u)$, with $\sigma_{old}(v) = 1 + \sigma(x)$.
 401 • $\sigma_{old}(y) = 1 + \sigma_{old}(v) + 1 + \sigma(u) = 3 + \sigma(x) + \sigma(u)$.
 402 • $\sigma_{new}(y) = 1 + \sigma_{new}(v) = 1 + \sigma_{old}(v) + 1 + \sigma(u) = 3 + \sigma(x) + \sigma(u) = \sigma_{old}(y)$.

403 So, the reconnection only increases the traffic load of node v , whereas the traffic load of the rest
 404 of nodes remains unchanged. Accordingly, the average traffic load of the layer containing node v
 405 increases, whereas the average traffic load of the rest of layers does not experience any change.
 406 Altogether, this means that the average traffic load calculated over the entire network increases for
 407 routing criteria that generate intra-layer connections.



408

409 **Figure 5.** Converting an inter-layer connection into an intra-layer (1) or a backward inter-layer (2)
 410 connection.

411 Let us focus now on the effects of backward inter-layer connections. Figure 5 shows an
 412 elementary change, where a (forward) inter-layer connection from node u to node y is replaced by
 413 a backward inter-layer connection to node x . The new balance is as follows:

- 414 • $\sigma_{new}(u) = \sigma_{old}(u) = \sigma(u)$.
 415 • $\sigma_{new}(x) = \sigma_{old}(x) + 1 + \sigma(u)$
 416 • $\sigma_{new}(v) = 1 + \sigma_{new}(x) = 1 + \sigma_{old}(x) + 1 + \sigma(u) = \sigma_{old}(v) + 1 + \sigma(u)$.
 417 • $\sigma_{old}(y) = 1 + \sigma_{old}(v) + 1 + \sigma(u)$.
 418 • $\sigma_{new}(y) = 1 + \sigma_{new}(v) = 1 + \sigma_{old}(v) + 1 + \sigma(u) = \sigma_{old}(y)$.

419 So, now the reconnection causes an increase in the traffic load of nodes x and v , whereas the
 420 traffic load of the rest of nodes remains unchanged. Accordingly, only the average traffic load
 421 supported by layers l_{i+1} and l_i increases, meaning that the average traffic load calculated over the
 422 entire network increases for routing criteria that generate backward inter-layer connections. In
 423 summary, any routing scheme generating intra-layer and/or backward inter-layer connections will
 424 incur an average traffic load larger than the average traffic load produced by a routing scheme that
 425 only generates (forward) inter-layer connections. *qed.*

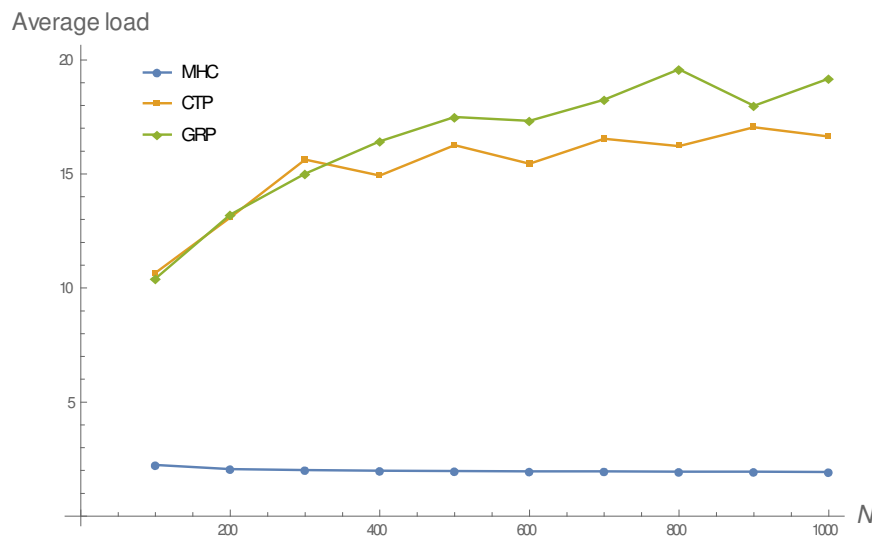
426 Note that creating a routing topology that only includes (forward) inter-layer connections is
427 equivalent to applying the minimum hop count criterion. Therefore, this is the optimal routing
428 strategy for time-driven duty-cycled EH-WSN under regular energy sources.

429 5. Numerical Results

430 In order to validate the theoretical results and demonstrate the impact of the routing strategy on
431 the average duty cycle of nodes, several simulation experiments were conducted by varying the
432 network size from 100 to 1000 sensor nodes (in steps of 100). The data shown in Table 1, which
433 correspond to TinyOS sensor nodes, were used. Correspondingly, the transmission range (r) was set
434 to 250 m. The sensor field consisted of a square region of 1 km², with the left lower corner and the
435 base station respectively located at coordinates (0,0) and (1000,500) (in meters). As for the
436 regular energy source, solar radiation was considered. The solar energy-harvesting model proposed
437 in [24] was used, with the meteorological data taken from the NASA POWER Project database for
438 the city of Madrid and the month of September: $D_{month} = 4.87$ kWh/m²/day and $STDHOURS = 12.5$
439 hours [25]. Three routing protocols were considered in the evaluation: the proposed Minimum Hop
440 Count (MHC)-based protocol, the well-known Collection Tree Protocol (CTP) and a location-based
441 or geographical routing protocol (GRP). CTP has been adopted in this evaluation as the best
442 representative of current routing protocols for EH-WSN, not only because of its extended use, but
443 also because it typically runs on top of a duty-cycled LPL-based MAC protocol (as in TinyOS-based
444 sensor networks). To be more precise, La-CTP should be considered, but the fact that a duty-cycled
445 LPL protocol is running at the MAC layer, there is no risk of loops and La-CTP would yield the same
446 results as CTP. In CTP, the expected number of transmissions (ETX) is adopted as the routing metric,
447 and then shortest path routing (SPR) is applied to determine the least cost path from every node to
448 the base station [26]. Note that the number of transmission tries is a magnitude that depends on both
449 the quality of the link that connects the two nodes and the asynchrony between their duty periods
450 (recall Figure 1). Since the purpose of this simulation is to compare the intrinsic effects of MHC, CTP
451 and GRP on the average traffic workload, it has been assumed that all feasible links are in good
452 quality conditions. Accordingly, the only factor determining the number of transmission tries is the
453 asynchrony between duty periods. As stated in [14], the number of transmission tries between a
454 transmitter and a receiver (parent) node is a fixed value extracted from a quasi-uniform distribution
455 between 1 and a maximum value that depends on the duty cycle of the receiver (parent) node. Note
456 that this introduces a “snake biting its tail” problem when dealing with CTP routing in the context of
457 EH-WSN, in which the duty cycle varies from node to node: the number of tries required by a given
458 node depends on the duty cycle of its parent node, which in turn depends on the routing topology
459 created by CTP based on the number of tries. In fact, this is a typical behavior observed in CTP: it
460 enters an initial transient period during which a connected network is progressively built, and after
461 that the routing topology becomes practically fixed, consistently with the regular traffic conditions
462 imposed by time-driven applications. In such a steady-state regime, the traffic load and duty cycle of
463 each node becomes stable, at least during long periods of time. Based on the data shown in Table 1,
464 the simulation experiments performed in [14] and the large network densities managed in the
465 current simulation (note that a large network density means a large number of nodes distributed
466 over a relatively small number of layers), a uniform distribution between 1 and 10 becomes
467 sufficiently representative to characterize the number of tries throughout all feasible links in the
468 network. Finally, another important category of routing protocols for sensor networks encompasses
469 those based on location information [27-28]. Though these protocols were developed for
470 battery-powered WSN, they could be perfectly extended to EH-WSN. In essence, these protocols
471 take advantage of location information to make routing more efficient. As indicated in [27], either
472 real or virtual geographical coordinates can be used (in the first case, sensor nodes are assumed to be
473 equipped with GPS). Protocols in this category use location information in multiple forms,
474 depending on how a node holding a packet selects the next-hop node in the route towards the
475 destination (base station). The neighbor which is closest (in terms of Euclidean distance) to the
476 destination, the most distant neighbor that is closer to the destination (most-forward-within-radius

477 technique), the nearest neighbor that is closer to the destination (nearest-forward-process) or the
 478 neighbor with the minimum angular distance from the imaginary line that connects the current node
 479 to the destination (compass routing), are just some examples. A common feature to these variations
 480 is that they introduce intra-layer connections that increase the average traffic workload over the
 481 network. Since this is the relevant fact in the present evaluation, a generic geographical routing
 482 protocol under the name of GRP has been simulated, leaving aside the specificities of each variation.
 483 Specifically, in GRP the next-hop node is randomly selected among all feasible intra-layer and
 484 forward inter-layer connections of the current node.

485 For each network size and routing protocol, the simulation experiment consisted of 30
 486 simulation runs, each providing two results: the average traffic load and the average duty cycle over
 487 the network. Particularly, Figure 6 shows the evolution of the average traffic load as the network size
 488 increases, for the three routing schemes considered in the analysis. As it can be noticed, MHC leads
 489 to significantly lower traffic load per node compared to the rest of routing criteria; this is because the
 490 latter generate intra-layer in addition to forward inter-layer connections, whereas the former only
 491 gives rise to forward inter-layer connections. Moreover, MHC also exhibits a practically flat behavior
 492 of around 2 forwarded packets per node on average, meaning that it is the routing metric that best
 493 distributes the overall traffic load across the network. Therefore, MHC is substantially more scalable
 494 in terms of network size than the rest of criteria.



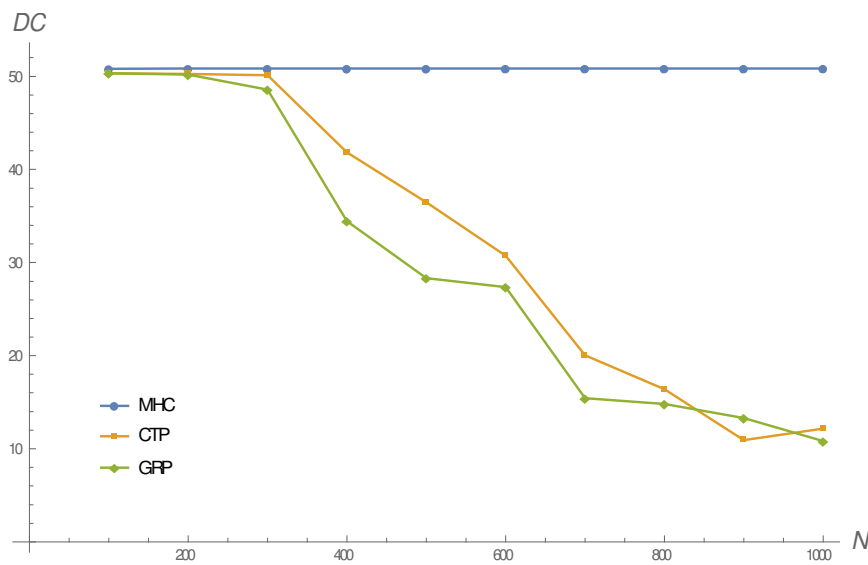
495

496 **Figure 6.** Evolution of the average traffic load with regard to the network size, for the routing metrics
 497 considered in the analysis. The surprisingly small value obtained for MHC is a consequence of the
 498 large network densities managed in the simulation.

499 The results in terms of the duty cycle of nodes are shown in Figure 7. This figure is a direct
 500 consequence of Figure 6 and Equation (13). Leaving aside the energy-harvesting term, Equation (13)
 501 defines the duty cycle of node X as a function of (1) the duty cycle of its parent node, through the
 502 term $E_{trigger}(X)$, and (2) the number of descendant nodes, through the term $\sigma(X)$. Accordingly,
 503 Algorithm 1 outlines the main steps to calculate the duty cycle of every node in the network. As it
 504 can be noticed, this algorithm proceeds by layers, though the concept of layer has been slightly
 505 modified here, since it is now based on the spanning tree that results from applying each routing
 506 metric. In other words, for a given spanning tree, the first layer is constituted by the nodes directly
 507 connected to the base station; the second layer contains the nodes directly connected to the nodes in
 508 the first layer; the third layer groups the nodes directly connected to the nodes in the second layer;
 509 etc. So, for instance, a node in the second layer could belong to the first layer according to the
 510 concept of layer adopted in Section 4.

511 As it can be noticed from Figure 7, all routing criteria give rise to very similar duty cycles
 512 (around 50%) for moderately large network sizes of up to 300 nodes approximately. However, as the

513 network size increases beyond this value, only MHC is capable of maintaining such a 50% duty
 514 cycle, whereas CTP and GRP exhibit highly-decreasing trends. Note that the gap between MHC and
 515 CTP might appear to be surprising, since CTP searches to minimize the link-level delay, which is
 516 also a consequence of the duty cycle maximization pursued by MHC. However, there is a subtle
 517 difference that explains this gap: CTP decides the next-hop neighbor based on the immediate
 518 number of transmission tries, fact that leads it to select intra-layer in addition to forward inter-layer
 519 connections. This behavior increases as the network size increases, and hence the decreasing trend
 520 shown in Figure 7. On the other hand, a small duty cycle has a negative impact on the whole
 521 distribution of the number of transmission tries, whose upper bound increases. So, indeed CTP
 522 selects the shortest routes based on the link-level delays, but these result from increasingly spread
 523 out distributions. In contrast, MHC selects exclusively forward inter-layer connections, which allows
 524 nodes to sustain large duty cycles even under increasing network sizes. Consequently, link-level
 525 delays in MHC-based routing obey distributions with smaller variances than those corresponding to
 526 CTP.



527

528

529

Figure 7. Evolution of the average duty cycle in terms of the network size, for different routing criteria.

530 **Algorithm 1: Evaluation of the duty cycle**

531 Let S be the given spanning tree (usually represented in matrix form).

532 From S , determine the set of layers $SL = \{layer_i, i = 1 \dots NL\}$, with NL the number of layers and
 533 $layer_i$ containing a subset of nodes. Note that $layer_i \cap layer_j = \emptyset \forall i \neq j$ and $layer_1 \cup \dots \cup$
 534 $layer_{NL} = U$, with U the whole set of sensor nodes in the network (universal set).

535 **for** $i = 1$ **to** $i = NL - 1$ **do**

536 Obtain the children nodes of every node $n_k \in layer_i$.

537 **for** $i = NL$ **downto** $i = NL - 1$ **do**

538 Calculate $\sigma(n_k)$ for every node $n_k \in layer_i$. Here, recall that $\sigma(X) = \sum_{i=1}^{CH(X)} \sigma(c_i(X))$. Note also
 539 that $\sigma(n_k) = 0 \forall n_k \in layer_{NL}$.

540 **for** $i = 1$ **to** $i = NL$ **do**

541 Obtain $DC(n_k)$ for every node $n_k \in layer_i$:

542 **if** $DC(p(n_k)) == 0$ **then** $DC(n_k) = 0$

543 **else**

544 Calculate $DC(n_k)$. Here, for $n_k \in layer_1$ it is assumed that the duty cycle of the base
 545 station is 100%.

546 **if** $DC(n_k) < 0$ **then** $DC(n_k) = 0$

547 Calculate the average duty cycle: $DC = \frac{1}{N} \sum_{n_k \in U} DC(n_k)$.

548 6. MHC in EH-WSN versus MHC in Battery-Powered WSN

549 Under the assumptions outlined in Section 1, the demonstration provided in this paper (Section
550 4) could be extended to battery-powered sensor networks if, additionally, all nodes were supplied
551 with the same initial amount of energy (otherwise, the optimal routing problem for such networks
552 would become NP-hard, as noticed in [29]). However, whereas the demonstration in Section 4 leads
553 to the conclusion that any MHC path maximizes the average duty cycle of nodes in an EH-WSN, it
554 would not suffice to determine the optimal routing strategy for battery-powered WSN with
555 homogeneous energy provision. The reason is that the optimal route for battery-powered WSN
556 under the previous assumptions is a MHC path, but not any MHC path. This is a consequence of the
557 “statistical” difference between the design objectives highlighted at the beginning of Section 1.
558 Additionally, we can outline other aspects related to the behavior of EH-WSN and battery-powered
559 WSN from the point of view of the application of the MHC routing strategy:

- 560 • The performance benefits derived from applying MHC to EH-WSN are much higher than those
561 obtained from applying the same routing strategy to battery-powered WSN. In effect, MHC for
562 EH-WSN does not only lead to the obvious minimization of path delay (in number of hops), but
563 it also reduces the link-level delay (under larger duty cycles, the number of transmission tries
564 from any node to its parent node is smaller) and increases the maximum throughput achievable
565 by the whole network (under smaller link-level delays, the number of packets that can be
566 forwarded by nodes during a reporting period is larger). Accordingly, MHC becomes more
567 scalable in terms of network size.
- 568 • As stated above, in battery-powered sensor networks with power control disabled, the optimal
569 routing solution is a specific MHC-based tree. However, this strategy is usually insufficient to
570 guarantee large network lifetimes due to the “black hole” problem (the node that supports
571 more traffic load experiences a rapid decay of its energy resources); accordingly, many
572 contributions in literature propose load balancing as an additional mechanism to prolong the
573 operational life of the sensor network. On the other hand, if power control is enabled, then
574 MHC is not necessarily the best choice, but again load balancing allows for extending network
575 lifetime. Examples of recent contributions on load balancing for battery-powered sensor
576 networks are [30-33]. These contributions typically rely on old well-known routing protocols
577 for sensor networks [34].
- 578 • As demonstrated in this paper, any MHC-based tree guarantees maximum average duty-cycle
579 of nodes in EH-WSN with power control disabled. Deviation from this routing strategy, either
580 to account for transmission distance in case power control is enabled or by introducing load
581 balancing, is not necessary unless a node is subject to very limited energy-harvesting
582 capabilities. This is explained by the fact that the duty cycles in EH-WSN are relatively large
583 and can be tuned according to the energy-harvesting capabilities of nodes. This contrasts with
584 the low flexibility exhibited by battery-powered WSN, in which minimized system-wide duty
585 cycles are always used.

586 7. Conclusions

587 In this paper, first a generic model has been developed to relate the duty cycle and traffic load
588 of any node in a time-driven duty-cycled EH-WSN. This model results from a relatively simple
589 extension of a previous result on the energy consumed by TinyOS nodes executing time-driven
590 applications. Then, the focus has been put on the routing strategy. Specifically, it has been
591 demonstrated that the MHC criterion minimizes the average traffic load across the network and
592 maximizes the average duty cycle of nodes. Note that this is a primary goal in energy-harvesting
593 WSN, since larger duty cycles are expected to optimize network performance.

594 The main result obtained in this paper has been validated via simulation by comparing MHC
595 with other relevant routing protocols, such as CTP and a generic geographic routing protocol (GRP)
596 (though any protocol that generated intra-layer connections would have served the same purposes).
597 Thus, this comparison encompasses three widespread and at the same time quite different routing

598 criteria for sensor networks: number of hops, number of transmission tries and geographical
599 distance. Simulations results reveal that MHC substantially outperforms the other protocols,
600 especially beyond moderately large network sizes. This also represents a better performance in
601 terms of scalability. Accordingly, this paper suggests assigning top priority to the MHC criterion in
602 the development of routing protocols for time-driven duty-cycled EH-WSN.

603 Also, a noticeable difference has been highlighted between EH-WSN and battery-powered
604 WSN regarding the application of the MHC routing strategy: whereas in EH-WSN any MHC-based
605 tree optimizes performance, in battery-powered WSN only a single MHC-based tree (or at most a
606 small subset of trees) optimizes network lifetime. This makes routing schemes for EH-WSN more
607 flexible than those for battery-powered WSN. Moreover, we can also expect that deviation from
608 MHC in EH-WSN does not become necessary unless some region of the sensor field is subject to
609 poor energy-harvesting conditions. However, this is an issue to be verified in further research:
610 what's the scope of MHC in time-driven EH-WSN when other conditions are taken into account:
611 power control enabled, transmission impairments, locally poor energy-harvesting situations and
612 even non-regular energy sources.

613 **Acknowledgments:** The solar irradiance data used in this paper were obtained from the NASA Langley
614 Research Center (LaRC) POWER Project funded through the NASA Earth Science/Applied Science Program.

615 **Conflicts of Interest:** The authors declare no conflict of interest.

616 References

- 617 1. Adu-Manu, K. S.; Adam, N.; Tapparello, C.; Ayatollahi, H.; Heinzelman, W. Energy-Harvesting Wireless
618 Sensor Networks (EH-WSNs): A Review. *ACM Transactions on Sensor Networks* 14, 2 (April 2018),
619 10:1-10:50.
- 620 2. Huang, P.; Xiao, L.; Soltani, S; Mutka, M. W.; Xi, N. The Evolution of MAC Protocols in Wireless Sensor
621 Networks: A Survey. *IEEE Communications Surveys & Tutorials* 15, 1 (First Quarter 2013), 101-120.
- 622 3. Sherazi, H. H. R.; Grieco, L. A.; Boggia, G. A Comprehensive Review on Energy Harvesting MAC
623 Protocols in WSNs: Challenges and Tradeoffs. *Ad Hoc Networks* 71 (March 2018), 117-134.
- 624 4. Pantazis, N. A.; Nikolidakis, S. A.; Vergados, D. D. Energy-Efficient Routing Protocols in Wireless Sensor
625 Networks: A Survey. *IEEE Communications Surveys & Tutorials* 15, 2 (Second Quarter 2013), 551-591.
- 626 5. Patil, M.; Biradar, R. C. A Survey of Routing Protocols in Wireless Sensor Networks. In Proceedings of the
627 2012 18th IEEE International Conference on Networks (ICON 2012). IEEE, New York, NY, USA, 86-91.
- 628 6. Lin, L.; Shroff, N. B.; Srikant, R. Asymptotically Optimal Energy-Aware Routing for Multihop Wireless
629 Networks with Renewable Energy Sources. *IEEE/ACM Transactions on Networking* 15, 5 (October 2007),
630 1021-1034.
- 631 7. Sun, G.; Shang, X.; Zuo, Y. La-CTP: Loop-Aware Routing for Energy-Harvesting Wireless Sensor
632 Networks. *Sensors* 2018, 18, 434, 1-20.
- 633 8. Wu, Y.; Liu, W. Routing Protocol Based on Genetic Algorithm for Energy Harvesting-Wireless Sensor
634 Networks. *IET Wireless Sensor Systems* 3, 2 (June 2013), 112-118.
- 635 9. Eu, Z. A.; Tan, H.-P.; Seah, W. K. G. Opportunistic Routing in Wireless Sensor Networks Powered by
636 Ambient Energy Harvesting. *Computer Networks* 54 (2010), 2943-2966.
- 637 10. Eu, Z. A.; Tan, H.-P. Adaptive Opportunistic Routing Protocol for Energy Harvesting Wireless Sensor
638 Networks. In Proceedings of the 2012 IEEE International Conference on Communications (ICC 2012).
639 IEEE, New York, NY, USA, 318-322.
- 640 11. Xiao, M.; Zhang, X.; Dong, Y. An Effective Routing Protocol for Energy Harvesting Wireless Sensor
641 Networks. In Proceedings of the 2013 IEEE Wireless Communications and Networking Conference
642 (WCNC 2013). IEEE, New York, NY, USA, 2080-2084.
- 643 12. Li, J.; Liu, D. An Energy Aware Distributed Clustering Routing Protocol for Energy Harvesting Wireless
644 Sensor Networks. In Proceedings of the 2016 IEEE/CIC International Conference on Communications in
645 China (ICCC 2016). IEEE, New York, NY, USA, 1-6.
- 646 13. Heinzelman, W. B.; Chandrakasan, A. P.; Balakrishnan, H. An Application-Specific Protocol Architecture
647 for Wireless Microsensor Networks. *IEEE Transactions on Wireless Communications* 1, 4, 660-670.
- 648 14. Galmés, S.; Escolar, S. Analytical Model for the Duty Cycle in Solar-Based EH-WSN for Environmental
649 Monitoring. *Sensors* 2018, 18, 2499, 1-32, DOI: 10.3390/s18082499.

- 650 15. Buettner, M.; Yee, G. V.; Anderson, E.; Han, R. X-MAC: A Short Preamble MAC Protocol for Duty-Cycled
651 Wireless Sensor Networks. In Proceedings of the 4th International Conference on Embedded Networked
652 Sensor Systems (SenSys 2006). ACM, New York, NY, USA, 307-320.
- 653 16. El-Hoiydi, A. Aloha with Preamble Sampling for Sporadic Traffic in Ad Hoc Wireless Sensor Networks. In
654 Proceedings of the 2002 IEEE International Conference on Communications (ICC 2002), vol. 5. IEEE, New
655 York, NY, USA, 3418-3423.
- 656 17. Polastre, J.; Hill, J.; Culler, D. Versatile Low Power Media Access for Wireless Sensor Networks. In
657 Proceedings of the 2nd International Conference on Embedded Networked Sensor Systems (SenSys 2004).
658 ACM, New York, NY, USA, 95-107.
- 659 18. Moss, D.; Levis, P. BoX-MACs: Exploiting Physical and Link Layer Boundaries in Low-Power
660 Networking. *Technical Report* SING-08-00. Stanford University, Palo Alto, CA, USA.
- 661 19. Musaloiu-E, R.; Liang, C. J. M.; Terzis, A. Koala: Ultra-Low Power Data Retrieval in Wireless Sensor
662 Networks. In Proceedings of the 2008 International Conference on Information Processing in Sensor
663 Networks (IPSN 2008). IEEE, New York, NY, USA, 421-432.
- 664 20. Sun, Y.; Gurewitz, O.; Johnson, D. B. RI-MAC: A Receiver-Initiated Asynchronous Duty Cycle MAC
665 Protocol for Dynamic Traffic Loads in Wireless Sensor Networks. In Proceedings of the 6th International
666 Conference on Embedded Networked Sensor Systems (SenSys 2008). ACM, New York, NY, USA, 1-14.
- 667 21. Dutta, P.; Dawson-Haggerty, S.; Chen, Y.; Liang, C. J. M.; Terzis, A. Design and Evaluation of a Versatile
668 and Efficient Receiver-Initiated Link Layer for Low-Power Wireless. In Proceedings of the 8th International
669 Conference on Embedded Networked Sensor Systems (SenSys 2010). ACM, New York, NY, USA, 1-14.
- 670 22. Kakria, A.; Aseri, T. C. A Survey on Asynchronous MAC Protocols in Wireless Sensor Networks.
671 *International Journal of Computer Applications* 108, 9, 19-22.
- 672 23. Kansal, A.; Hsu, J.; Zahedi, S.; Srivastava, M. B. Power Management in Energy Harvesting Sensor
673 Networks. *ACM Transactions on Embedded Computing Systems* 6, 4 (September 2007), 32:1-32:38.
- 674 24. Escolar, S.; Chessa, S.; Carretero, J. Energy Management in Solar Cells Powered Wireless Sensor Networks
675 for Quality of Service Optimization. *Personal Ubiquitous Computing* 18, 2 (February 2014), 449-464.
- 676 25. NASA POWER Project Data Sets. <https://power.larc.nasa.gov/data-access-viewer>.
- 677 26. Gnawali, O.; Fonseca, R.; Jamieson, K.; Moss, D.; Levis, P. Collection Tree Protocol. In Proceedings of the
678 7th ACM Conference on Embedded Networked Sensor Systems (SenSys '09), Berkeley, CA, USA, 4-6
679 November, 2009; pp. 1-14.
- 680 27. García-Villalba, L. J.; Sandoval-Orozco, A. L.; Triviño-Cabrera, A.; Barenco-Abbas, C. J. Routing Protocols
681 in Wireless Sensor Networks. *Sensors*, 2009, 9, 8399-8421, DOI: 10.3390/s91108399.
- 682 28. Karl, H.; Willig, A. *Protocols and Architectures for Wireless Sensor Networks*. John Wiley & Sons: Chichester,
683 West Sussex, UK, 2005.
- 684 29. Wu, Y.; Fahmy, S.; Shroff, N. B. On the Construction of a Maximum-Lifetime Data Gathering Tree in
685 Sensor Networks: NP-Completeness and Approximation Algorithm. In Proceedings of IEEE INFOCOM
686 2008, Phoenix, AZ, USA, 13-18 April, 2008; pp. 1013-1021.
- 687 30. Kacimi, R.; Dhaou, R.; Beylot, A.-L. Load Balancing Techniques for Lifetime Maximization in Wireless
688 Sensor Networks. *Ad Hoc Networks*, 2013, 11, 2172-2186.
- 689 31. Zhang, D.; Li, G.; Zheng, K.; Ming, X.; Pan, Z.-H. An Energy-Balanced Routing Method Based on
690 Forward-Aware Factor for Wireless Sensor Networks. *IEEE Transactions on Industrial Informatics*, 2014, 10,
691 1, 766-773.
- 692 32. Kleerekoper, A.; Filer, N.P. DECOR: Distributed Construction of Load Balanced Routing Trees for Many to
693 One Sensor Networks. *Ad Hoc Networks*, 2014, 16, 225-236.
- 694 33. Liu, X.; Zhang, P. Data Drainage: A Novel Load Balancing Strategy for Wireless Sensor Networks. *IEEE*
695 *Communications Letters*, 2018, 22, 1, 125-128.
- 696 34. Akkaya, K.; Younis, M. A Survey on Routing Protocols for Wireless Sensor Networks. *Ad Hoc Networks*,
697 2005, 3, 325-349.